Mathematical Biosciences and Engineering

http://www.aimspress.com/journal/MBE

MBE, 18(1): 300–304.
DOI: 10.3934/mbe.2021015
Received: 18 November 2020
Accepted: 20 November 2020
Published: 27 November 2020

Correction

Correction: A comparative analysis of noise properties of stochastic binary models for a self-repressing and for an externally regulating gene

Guilherme Giovanini[1], Alan U. Sabino[2], Luciana R. C. Barros[3] and Alexandre F. Ramos[1,2,*]

[1] Escola de Artes, Ciências e Humanidades, Universidade de São Paulo, Av. Arlindo Béttio, 1000, 03828-000, São Paulo, Brazil

[2] Instituto do Câncer do Estado de São Paulo, Faculdade de Medicina, Universidade de São Paulo, Av. Dr. Arnaldo, 251, 01246-000, São Paulo, Brazil

[3] Fundação Faculdade de Medicina, Faculdade de Medicina, Universidade de São Paulo, Av. Rebouças, 381, 05401-000, São Paulo, Brazil

* **Correspondence:** Email: alex.ramos@usp.br; Tel: +551130911235.

A correction on

A comparative analysis of noise properties of stochastic binary models for a self repressing and for an externally regulating gene by Guilherme Giovanini, Alan U. Sabino, Luciana R. C. Barros and Alexandre F. Ramos. Mathematical Biosciences and Engineering 2020, 17(5): 5477–5503. doi:10.3934/mbe.2020295.

We would like to submit the following corrections to our recently published paper [1] due to the use of incorrect data files to build two of the graphs contained in the manuscript. We also corrected some typos in the text that describe the statistical values related to the graphs mentioned. Additionally, we uploaded a verification code to our Laboratory's GitHub repository (https://github.com/amphybio/Giovanini2020_ComparativeAnalysis) to enable the reproduction of our numerical calculations by the interested readers. The details are the following.

1. The Figures 3B and 4B, and their respective captions have been updated.

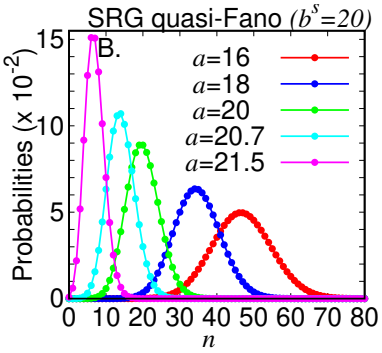

Figure 3. We consider probability distributions denoted Fano ($\mathcal{F} = 1$) or quasi-Fano ($\mathcal{F} \approx 1$). The graphs for the SRG have $z_0 = 0.9$. Graph A has strictly Fano distributions and for the condition $a = b^s$ the moments of the distributions are $(\mathcal{F}^s, \xi^s, \langle n^s \rangle, p^s_\alpha) = (1, 0, b, z_0)$. Graph B has quasi-Fano distributions for SRG which moments are presented in increasing order of a as shown in legend: $\mathcal{F}^s \approx$ (1.4, 1.1, 1, 0.98, 0.98); $\xi^s \approx$ (17.5, 4.7, 0, −0.3, −0.2); $\langle n^s \rangle \approx$ (47, 35, 20, 14, 7); $p^s_\alpha \approx$ (0.75, 0.82, 0.9, 0.93, 0.97). Graph C has quasi-Fano distributions for ERG with $N = 50$. The moments of the distributions are presented in increasing order of a as shown in legend: $\mathcal{F}^e \approx$ (1.3, 1.2, 1.1, 1.0, 1); $\xi^e \approx$ (9.9, 7.8, 5.2, 1.9, 0); $\langle n^e \rangle \approx$ (36, 40, 44, 48, 50); $p^e_\alpha \approx$ (0.72, 0.80, 0.88, 0.96, 1).

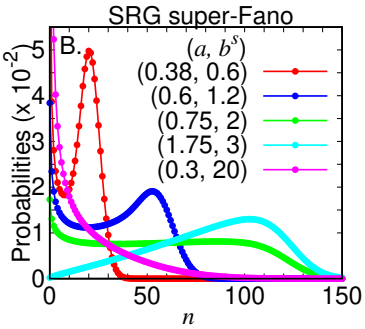

Figure 4. We consider super-Fano probability distributions ($a < b$). In Graph A (SRG) the parameters are indicated inside graph and the moments of the distributions are given in the same order of the values for pairs (a, z_0) within the graph: $\mathcal{F}^s \approx$ (9.8, 14.7, 21.3, 11.2, 7.8); $\xi^s \approx$ (472.3, 808.4, 1225.9, 310.5, 139.8); $\langle n^s \rangle \approx$ (53.7, 58.9, 60.4, 30.5, 20.5); $p^s_\alpha \approx$ (0.66, 0.58, 0.50, 0.49, 0.49). In Graph B (SRG) z_0 is 0.99 for the four smallest values of b^s and for the remaining one value of b^s we have $z_0 = 0.9$. The moments are presented in increasing order of b^s: $\mathcal{F}^s \approx$ (5.6, 13.8, 23.5, 11.3, 25.9); $\xi^s \approx$ (69.0, 405.2, 1339.0, 857.9, 352.6); $\langle n^s \rangle \approx$ (15, 34, 60, 83, 14); $p^s_\alpha \approx$ (0.66, 0.56, 0.47, 0.65, 0.065). Graph C has super-Fano distributions for ERG with $N = 50$. The moments of the distribution are presented in increasing order of a: $\mathcal{F}^e \approx$ (14.3, 13.5, 9.3, 7.3, 3.2); $\xi^e \approx$ (400, 312.5, 208.3, 156.3, 9.3); $\langle n^e \rangle \approx$ (30, 25, 25, 25, 4.3); $p^e_\alpha \approx$ (0.6, 0.5, 0.5, 0.5, 0.085).

2. The second and fourth paragraphs in Section 3.3 have been updated.

Figure 4, Graph A has five probability distributions. The distributions displayed in magenta and cyan are bimodal. The green line shows a distribution approximately like a table. The blue and red lines indicate single modal widespread distributions because of the significant probability of finding from zero to ≈ 100 proteins while their averages are ≈ 50. Figure 4, Graph B shows two bimodal probability distributions, shown in blue and red. The distribution in green is table-shaped and the one in cyan is a single modal and in both there are significant probabilities of finding from 0 to ≈ 130 proteins. The magenta distribution can be approximated as a negative binomial distribution which is a typical distribution when one has transcriptional or translational bursts [50, 57]. Figure 4, Graph C shows super-Fano distributions for the ERG. We assume a fixed value for N and change values of b^e considering some values for a that permit us to generate probability distributions that are widespread. The red and blue distributions are bimodal with modes centered around 50 and 0. The green distribution is table shaped such that there is a significant probability of finding from zero to a bit beyond N proteins. The cyan distribution is one modal and it is widespread, similarly to the table-shaped distribution. Finally we have the magenta distribution which is approximated by a negative binomial.

The super-Fano distributions of Graph A have the OFF to ON switching rate of the order of 10^{-2} min^{-1} which is the same order of the effective ON to OFF switching rate, $\frac{hk}{\rho+h}$ [23] and of the degradation rate of the proteins. That causes the probability distributions to be bi-peaked as the biochemical processes are slower. The super-Fano distributions of Graph B have the effective ON to OFF switching rate given in min^{-1} approximated by $(2 \times 10^{-3}, 6 \times 10^{-3}, 10^{-2}, 10^{-2}, 0.2)$ presented in increasing order of N. For the maximal N the effective rate of ON to OFF switching is almost a hundred times larger than the corresponding OFF to ON switching rate. Note that the synthesis rate a hundred times larger than the degradation, which can be considered as a very efficient protein production process. At that limit the promoter remains mostly OFF and the distribution approaches a negative binomial as occurs in bursty protein synthesis [50]. The super-Fano distributions of Graph C show that the stochastic binary model for the ERG having kinetic parameters of the same order as that for a SRG will generate proteins governed by similar probability distributions. That similarity may become a confusing element on the inference of gene regulation based on noise in gene expression. Perhaps, this problem is only theoretical significance, if the differences on the probability distributions generate fluctuations on protein numbers lying within the detection limits of biological systems. About 40% of *E. coli* genes are self-repressed [30] and it would be interesting to determine whether this is because of the wider possibility of ranges of stochastic gene expression regimes enabled by the SRG or if a downstream regulated gene can detect the particularities on the fluctuations of the protein numbers generated by either the ERG or SRG.

3. The Tables 1 and 2 have been updated.

Table 1. Approximated values of the kinetic parameters on Figure 4.

Graph A (N, k, f, h)	Graph B (N, k, f, h)	Graph C (k, f, h)
$(80, 0.8, 10^{-2}, 10^{-4})$	$(20, 0.2, 4 \times 10^{-3}, 10^{-4})$	$(0.5, 3 \times 10^{-3}, 2 \times 10^{-3})$
$(100, 1, 10^{-2}, 10^{-4})$	$(60, 0.6, 6 \times 10^{-3}, 10^{-4})$	$(0.5, 5 \times 10^{-3}, 5 \times 10^{-3})$
$(100, 1, 8 \times 10^{-3}, 10^{-4})$	$(130, 1.3, 8 \times 10^{-3}, 10^{-4})$	$(0.5, 10^{-2}, 10^{-2})$
$(60, 0.6, 8 \times 10^{-3}, 2 \times 10^{-4})$	$(130, 1.3, 2 \times 10^{-2}, 10^{-4})$	$(0.5, 1.5 \times 10^{-2}, 1.5 \times 10^{-2})$
$(40, 0.4, 8 \times 10^{-3}, 3 \times 10^{-4})$	$(220, 2.2, 3 \times 10^{-3}, 10^{-3})$	$(0.5, 0.017, 0.183)$

Table 2. Values of the kinetic parameters on Figure 5A.

b^s	Sub-Fano $(N, k, f, K = h/f)$	Fano $(N, k, f, K = h/f)$
0.5	(167.1, 1.7, 8.3, 2.4)	$(10^3, 10.0, 5 \times 10^{-3}, 4 \times 10^3)$
1	(333.2, 3.3, 16.7, 1.2)	$(2 \times 10^3, 20.0, 10^{-2}, 2 \times 10^3)$
2	(667.3, 6.7, 33.3, 0.6)	$(4 \times 10^3, 40.0, 2 \times 10^{-2}, 10^3)$
3	(1000.5, 10.0, 50.0, 0.4)	$(6 \times 10^3, 60.0, 3 \times 10^{-2}, 7 \times 10^2)$
4	(1333.7, 13.3, 66.7, 0.3)	$(8 \times 10^3, 80.0, 4 \times 10^{-2}, 5 \times 10^2)$

4. The second paragraph in Section 3.4 has been updated.

In the Table 2, the parameter values generating the probability distributions of Graph A are rewritten in terms of the kinetic constants in Eqs (2.1)–(2.4). A fixed $z_0 = 5 \times 10^{-4}$ implies a $h \sim 20$ min^{-1} if we assume $\rho = 0.01$ min^{-1}. For each pair of sub-Fano and Fano probability distributions having the same average, a pair (a, b^s) results on the following approximate values of the kinetic parameters, where k and f are given in min^{-1} and K indicates the equilibrium binding affinity of the regulatory protein. The order of K for the sub-Fano distributions are $K \sim 1$ while they are of the order of 10^3 on the Fano ones. The OFF to ON switching rates on the sub-Fano distributions are typically a hundred times faster than those of the Fano ones. On the other hand, the effective ON to OFF switching rate, $\frac{hk}{\rho+h}$, given in min^{-1} for the sub-Fano and the Fano distributions are approximately (1.7, 3.3, 6.7, 10, 13.3) and (10., 20., 40., 60., 80.), respectively, for each value of b^s given in crescent order accordingly with the captions. Therefore, the effective ON to OFF switching rate is almost ten times faster on the Fano distributions. When we compare effective switching rates between the two promoter states, we note that the sub-Fano processes have an $\sim$ 10× faster OFF to ON transition while it is $\sim 10^{-3}\times$ slower for Fano ones. That causes the ON state probabilities in the sub-Fano regime, and hence the duration of the ON state, to be about a hundred times longer than in the Fano one. The synthesis rate values provide the compensatory effect to ensure that the two noise regimes will have the same average number of products. Graph C shows that the asymptotic Fano factor for the sub-Fano regime happens for a wide range of values of average protein numbers. Graph B shows that the asymptotic Fano factor happens for smaller ON state probabilities in combination with larger values of the synthesis rate.

This parameter regime of SRG is qualitatively distinct from the ERG, as the latter would be in the bursty limit of gene expression [50].

5. The Eq (A.7) has been updated.

$$\langle n_\alpha^s \rangle = \frac{a}{b^s}\frac{z_0}{c}\frac{1}{1-z_0}\left[b^s \mathrm{M}(a, b^s, Nz_0(1-z_0)) - (b^s - Nz_0(1-z_0))\mathrm{M}(a+1, b^s+1, Nz_0(1-z_0))\right].$$

These errors do not change the interpretation of our results. We apologize for any inconvenience caused to the readers.

References

1. G. Giovanini, A. U. Sabino, L. R. C. Barros, A. F. Ramos, A comparative analysis of noise properties of stochastic binary models for a self-repressing and for an externally regulating gene, *Math. Biosci. Eng.*, **17** (2020), 5477–5503.

AIMS Press